Ab Initio Calculation of the Crystalline Structure and IR Spectrum of Polymers: Nylon 6 Polymorphs

Claudio Quarti,[†] Alberto Milani,*,[†] Bartolomeo Civalleri,[‡] Roberto Orlando,[‡] and Chiara Castiglioni[†]

[†]Dipartimento di Chimica, Materiali e Ingegneria Chimica "G. Natta", Politecnico di Milano, Piazza Leonardo da Vinci 32, I-20133 Milano, Italy

[‡]Dipartimento di Chimica e Centro di Eccellenza NIS, Università di Torino, Via P. Giuria 7, I-10125 Torino, Italy

Ⓢ *Supporting Information*

ABSTRACT: State-of-the-art computational methods in solid-state chemistry were applied to predict the structural and spectroscopic properties of the α and γ crystalline polymorphs of nylon 6. Density functional theory calculations augmented with an empirical dispersion correction (DFT-D) were used for the optimization of the two different crystal structures and of the isolated chains, characterized by a different regular conformation and described as one-dimensional infinite chains. The structural parameters of both crystalline polymorphs were correctly predicted, and new insight into the interplay of conformational effects, hydrogen bonding, and van der Waals interactions in affecting the properties of the crystal structures of polyamides was obtained.

The calculated infrared spectra were compared to experimental data; based on computed vibrational eigenvectors, assignment of the infrared absorptions of the two nylon 6 polymorphs was carried out and critically analyzed in light of previous investigations. On the basis of a comparison of the computed and experimental IR spectra, a set of marker bands was identified and proposed as a tool for detecting and quantifying the presence of a given polymorph in a real sample: several marker bands employed in the past were confirmed, whereas some of the previous assignments are criticized. In addition, some new marker bands are proposed. The results obtained demonstrate that accurate computational techniques are now affordable for polymers characterization, opening the way to several applications of ab initio modeling to the study of many families of polymeric materials.
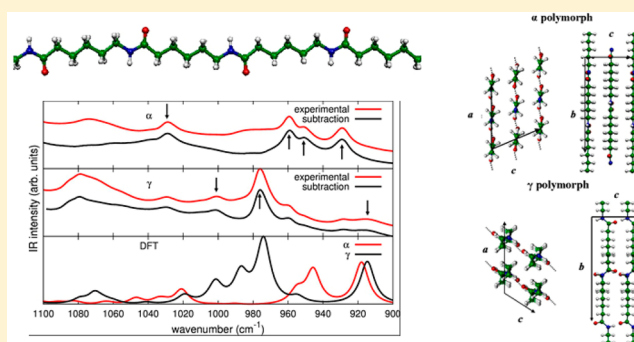
I. INTRODUCTION

Polyamides, commonly known by the commercial name nylon, are well-recognized polymeric materials, because of their wide occurrence in everyday life. Despite their well-assessed applications, scientific and technological research on this class of polymers is far from having reached a plateau: The development of nanocomposites based on nylons,[1] the application of new techniques of production such as electrospinning,[2] and even the application of polyamides in the field of biomaterials and nanomedicine are currently active and promising fields of investigation.

From a more basic, physicochemical point of view, the development of structure/property relationships based on a molecular approach and the understanding of the origin of the polymorphism that arises in several semicrystalline polyamides are currently being deeply investigated both experimentally[2f,3] and theoretically;[4] in particular, thanks to the development of molecular simulations and related computational techniques, ab initio theoretical modeling can be exploited to this aim.

Polymorphism is one of the key features ruling, at the nanoscale, the properties of polyamides; however, despite its importance, the control and experimental recognition of the crystalline structure of nylons are issues that have not been completely solved. The existence of metastable phases, the peculiar behavior observed upon thermal or mechanical stresses, the phenomena ruling the stability of one phase or another, and the understanding of phase transitions from a molecular perspective are just a few topics about which many questions are still unanswered. The complexity of this matter arises from the peculiar balance between intra- and intermolecular interactions taking place in these systems. For instance, in the case of single-numbered nylons (nylon n, where n is even), the stability of the α crystalline form with respect to the γ form depends on the length of the monomer chain (i.e., on the number of $-CH_2$ units). Indeed, the balance between intermolecular H-bonding and van der Waals (vdW) interactions among $-CH_2-$ units belonging to adjacent chains in the crystal determines the predominance of one form or the other.[4a] In particular, the α form is more stable for $n \leq 6$, whereas the γ form is more stable for $n \geq 8$. The case of nylon 6 (NY6) is most peculiar because it presents both crystal forms, often occurring simultaneously in the same sample, because of

the small difference in energy between them, with the α form being more stable. In addition, this polymer can easily undergo a phase transition from the α to the γ form as a result of external stimuli or processing.[2b,3e,i,5]

Because the setting of a given crystal structure implies peculiar trends of the macroscopic properties (e.g., melting temperatures, densities, mechanical properties), a careful determination of the crystal structure is mandatory and has been widely carried out by means of X-ray diffraction and IR spectroscopy.[2b,3i,5,6]

In parallel, calculations based on molecular dynamics[4a,7] have been used to investigate the structural properties of nylons, together with quantum chemical simulations carried out on feasible small molecular models.[4b] However, because of the limited computational resources and the lack of standard codes, any accurate quantum chemical calculations of infinite polymer chains and their crystal structures were unaffordable in the past. Even if a very good computational description of the molecular structure could be obtained by means of classical molecular dynamics,[7] these methods do not allow the prediction of reliable vibrational spectra. On the other hand, ab initio molecular dynamics techniques can, in principle, give a very good description of the vibrational force field and spectra of quite large molecular systems, provided that the simulations are long enough for reliable statistics to be obtained. Anharmonic effects can be automatically included in these calculations, but on the other hand, a description of the vibrational properties in terms of normal modes is not straightforward. Recently, these methods have been applied successfully to different molecular systems,[8] but they have not found application yet in the case of polymeric materials, which are still too computationally expensive. So far, indeed, very few works have been published on the computational vibrational spectroscopy of polyamides, and they were all based on semiempirical force fields.[9]

Because of this lack, the characterization of nylons by means of vibrational spectroscopy has always relied on band assignments based on purely experimental works:[5,6,9] The diagnostic tools so developed are now routinely used for the spectroscopic characterization of new systems such as nano-composites or electrospun nanofibers as well. Unfortunately, the reliability of these assignments has not be confirmed through accurate molecular modeling.

In this article, we present a computational study based on density functional theory (DFT) calculations of the IR spectra of the α and γ crystalline forms of NY6 using state-of-the-art computational techniques in solid-state chemistry. Indeed, in the current implementation of the CRYSTAL09 code,[10] accurate simulation of the vibrational properties of crystalline molecular materials is possible, explicitly taking into account the space group symmetry of the systems. In the case of polymeric materials, accurate calculations using this code have recently been presented and applied with success to the case of a single chain of syndiotactic polystyrene,[11] polyglycine,[12] and a few polyconjugated polymers.[13] To our knowledge, however, no other application of this code to the study of polymer materials has been presented so far.

The work is organized as follows: In section III.1, the DFT-computed equilibrium structures of the two α and γ crystalline forms of NY6 are compared with experimental determinations, focusing in particular on the importance of van der Waals interactions and the effects of their correction by means of Grimme's procedure. The structural results obtained were then used in the simulation of the IR spectra described in section

III.2. The interpretation of the IR spectra and the assignment of the spectroscopic markers of α and γ polymorphs of NY6 are reported in section IV.

II. COMPUTATIONAL AND EXPERIMENTAL DETAILS

Full geometry optimization of the crystal structures and calculation of the IR spectra of the α and γ polymorphs of NY6 were carried out by means of the CRYSTAL09 code[10] within the framework of density functional theory (DFT). We employed the B3LYP[14] hybrid exchange-correlation functional together with the 6-31G(d,p) basis set. (The dimensions of the basis set are reported in the Supporting Information, together with the atoms and fractional coordinates of the asymmetric unit of the optimized structures.)

All B3LYP calculations included the empirical correction for dispersion interactions proposed by Grimme[15] and implemented in CRYSTAL09. Three different sets of empirical parameters were used and compared because it has been demonstrated in previous works[16] that the results could be significantly affected by different choices. The numerical values of the parameters finally chosen in this work are reported in Table 1. Further details and comments about this choice are reported in the Supporting Information.

Table 1. Summary of the C_6 and R_{vdW} Parameters Employed in the Present Work for the Grimme Correction[15,a,b]

atom	C_6^{15} (J nm^6 mol^{-1})	R_{vdW} (Å)
H	0.14	1.3013[16]
C	1.75	1.70[17]
O	0.70	1.52[17]
N	1.23	1.55[17]

[a]Cutoff distance of 25.0 Å used to truncate direct lattice summation. [b]Standard values of $d = 20$ and $s_6 = 1.00$ used.[16]

In all calculations, the atomic positions and the lattice parameters were fully optimized; default optimization algorithms and convergence criteria were employed.[10a]

As starting guess structures for the calculations, we considered the experimentally determined crystal parameters and atomic coordinates reported by Holmes et al.[18a] and Simon et al.[18b] for the α form ($P2_1$ space group) and by Arimoto et al. for the γ form ($P2_1/a$).[19] To detect the spectroscopic markers of regularity/crystallinity,[20] we carried out geometry optimizations and frequency calculation on the infinite polymer chain characterized by a regular conformation (one-dimensional model chain), taking as starting structures the two different conformations shown by the chains in the two polymorphs: The "α-type" chain belongs to $P2_1am$ line group and is characterized by a transplanar structure, whereas the "γ-type" chain belongs to the $P2_111$ line group and shows a nonplanar arrangement of the backbone atoms, determined by the skew conformation of the CH_2 units adjacent to the amide group.

The two crystal structures, showing the two different conformations of the polymer chains, are sketched in Figure 1.

Calculations of normal frequencies (at the Γ point) were carried out on the optimized geometries as obtained by diagonalization of the (numerically calculated) Hessian matrix.

Vibrational frequencies and eigenvectors obtained for the one-dimensional model chains were used for the interpretation of the normal modes of vibration observed in the crystal, according to a "projection" procedure reported in section IV.
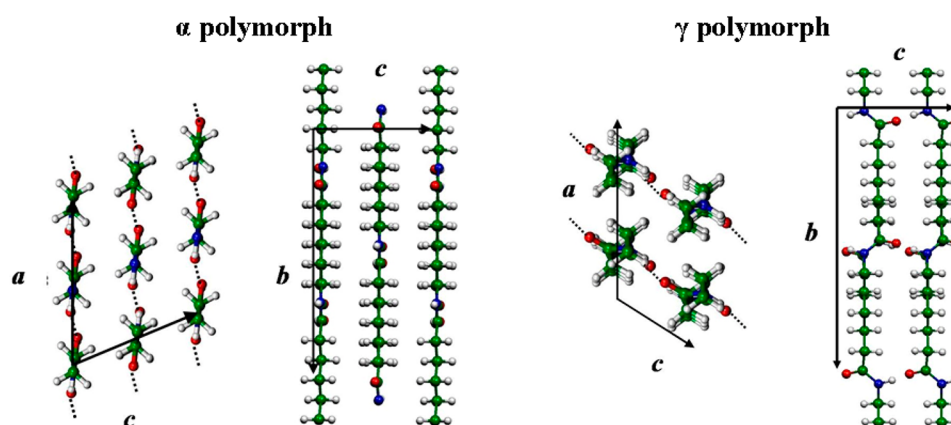
Figure 1. Sketches of the crystalline structures of the α and γ polymorphs of NY6. Carbon atoms are in green; hydrogen atoms, white; oxygen atoms, red; and nitrogen atoms, blue.

To compare the computed and experimental data, the calculated frequencies were scaled by 0.9614[21] in the frequency range of 4000−1100 cm^{-1} and by 0.975 below 1100 cm^{-1}. Different scaling factors were used here to obtain the best fit between the experimental and computed IR spectra.

The DFT-D-computed spectra were compared with experimental IR spectra of two different NY6 samples showing large excess contents of the α and γ crystalline polimorphs and with an amorphous sample.[22] Samples of α crystals with a thickness suitable for IR analysis were prepared starting from formic acid solution of NY6 and coating a film by means of the Doctor Blade technique. Samples of the γ form were prepared following the procedure previously reported in the literature.[3i,22,23] IR spectra were recorded using an FT-IR Nicolet Nexus Spectrometer (resolution 1 cm^{-1}, 128 scans). Amorphous samples were obtained by rapid quenching of the melt in liquid nitrogen. All experimental spectra reported showed good agreement with the experimental spectra previously published in the literature and can be used for a reliable validation and discussion of the DFT-D-predicted spectra. In the case of the γ form, the IR spectra show very weak bands, which can be associated to the presence of slight impurities of the α form. Anyway, their content is very limited and does not affect the comparison with the predicted spectra.

III. RESULTS

III.1. Prediction of the Crystal Structures. The correct prediction of the crystal structure and of the cohesive energy of NY6 polymorphs is a computationally difficult task. As already mentioned, the intermolecular properties of single-numbered nylons are ruled by the interplay between hydrogen-bonding and vdW interactions among >CH$_2$ groups, stabilizing the α or the γ crystalline form depending on the length of the monomer chain. The computational description of these interactions is currently one of the weaknesses of the DFT method in the case of small molecules as well, but it can be corrected by the empirical procedure proposed by Grimme,[15] employed herein. Furthermore, the computational difficulties parallel the experimental problems related to the existence (or coexistence) of other polymorphs in addition to the α and γ phases and of the unavoidable presence of the amorphous phase, as always occurs for any semicrystalline polymer. These facts add further uncertainties in the interpretation of experimental measures, as documented by the wide debate on the crystalline structures of NY6 that took place in the past literature.[5,6]

In this work, we restrict ourselves to the modeling of the structures of the two main (α and γ) crystalline forms of NY6, by comparing them to the experimental structures reported by Holmes et al. and Simon and Argay[18] and by Arimoto et al.:[19] these structures are indeed referred to by most of the scientific articles dealing with NY6.

In Table 2, we report a comparison between the experimental cell parameters and those computed using the

Table 2. Experimental[18,19] and DFT-D-Computed Cell Parameters for α and γ Forms of NY6

	α polymorph ($P2_1$)		γ polymorph ($P2_1/a$)	
	expt[18]	DFT-D	expt[19]	DFT-D
a (Å)	9.56	9.57	9.33	8.99
b (Å)	17.24	17.48	16.88	16.85
c (Å)	8.01	7.53	4.78	4.75
β (deg)	67.5	68.64	121.0	123.3

set of parameters for the Grimme correction reported in Table 1. A complete discussion of the results obtained using other different sets of parameters is provided in the Supporting Information.

Considering first the results for the α form, good predictions were found for the β angle and b parameter (chain axis direction), consistent with the fact that the latter cell parameter depends on the good computational description of the intramolecular degrees of freedom. The a parameter is related to the packing between neighboring hydrogen-bonded chains forming a sheet (see Figure 1). Very good agreement with experimental data was obtained in this case as well, indicating that hydrogen-bonding effects are described properly by the computational method employed. The largest discrepancy with the experimental data was found for the c parameter, related to the packing of "sheets" (formed by H-bonded chains) interacting through vdW forces: The set of parameters employed (Table 1) was the one giving the best agreement (see the Supporting Information), even though a non-negligible difference from the experimental determination was still present. For the γ form, a very similar situation was found: The b parameter (chain axis), the β angle, and the c parameter (H-bonded chains in pleated sheets) were described accurately, and a good description was obtained for the a parameter (stacking of sheets through vdW interactions), even though a

non-negligible difference was still found with respect to the experimental value.

However, on one hand, in the case of molecular solids, thermal effects can have a non-negligible role in modulating this cell parameter,[24] and a comparison with the result of a complete cell optimization by means of ab initio calculations should be undertaken with care because no thermal effects are included in the latter. On the other hand, the slight underestimation can be due to a basis set incompleteness that causes a spurious extra-binding due to basis set superposition error (BSSE) that adds to the genuine attractive dispersion correction. The employed set of parameters, in particular the use of Bondi's van der Waals radii, probably leads to an error cancellation between the two contributions that provides the best prediction of the lattice parameters (see the Supporting Information).

One can thus conclude that a reasonably good description of the crystal structure of NY6 polymorphs can be obtained by using the selected parameters employed for the Grimme correction (see Table 1), justifying their use also for the computation of the IR spectra of the two polymorphs.

A very important feature for the comprehension of the polymorphism in NY6 is the relative stability of one crystalline form with respect to the other. To date, very few works based on molecular mechanics[7] or quantum chemical calculations applied to small molecular models[4b] have been used for this purpose, and the general conclusion was that the α form is more stable than the γ form, showing an energy difference of 0.5−1.5 kcal/mol per monomer unit, depending on the computational method employed. Because in the present work our aim is a detailed description and discussion of structure and vibrational features of the two polymorphs, a complete investigation of the energetics behind nylon's polymorphism is planned for the near future. We just briefly summarize some preliminary results here.

It is interesting to compare the energy differences between the two isolated polymer chains (one-dimensional model chains), exhibiting conformations very similar to those observed when forming the crystal, to determine the contribution of the conformational potential energy for the two different chains. Grimme's correction has also been used in this case to guarantee the best description of the interactions between nonbonded atoms, playing a significant role in determining the shape of the torsional potential surface.

If one uses the molecular structure of a single polymer chain "extracted" from the experimental crystal structures as a guess geometry and carries out a complete geometry optimization (no constraints except for the choice of symmetry rod group, which does not affect the final value of the torsional angles), the two starting conformations are kept (except for an expected and small geometry relaxation). This is a first very interesting result: it suggests that the two chain conformations characteristic of the α and γ forms are not driven by the intermolecular interactions but also satisfy equilibrium requirements for the isolated chain (i.e., they correspond to minima of the torsional potential energy surface of the single polymer chain). The energy difference between the two conformations of the isolated chains (normalized on the monomer units) demonstrates that the γ-type conformation is slightly more stable (1.073 kcal/mol) than the α-type conformation whereas, in the crystals, the two polymorphs are practically isoenergetic (energy difference of 0.045 kcal/mol per monomer unit). On the other hand, the α form is slightly more stable (up to a

maximum of 1.5 kcal/mol per monomer unit) if other sets of parameters for Grimme's correction are used (see Table S3 of the Supporting Information). These preliminary and qualitative results are particularly interesting because they show how polymorphism in nylon 6 results from a subtle balance of both intra- and intermolecular interactions, requiring an accurate computational description of both of these types of interactions.

III.2. IR Spectra of NY6 Polymorphs. In this section, the IR spectra obtained by DFT-D calculations are presented and compared to the experimental spectra of the two polymorphs. In Figure 2, the computed and experimental spectra for the two
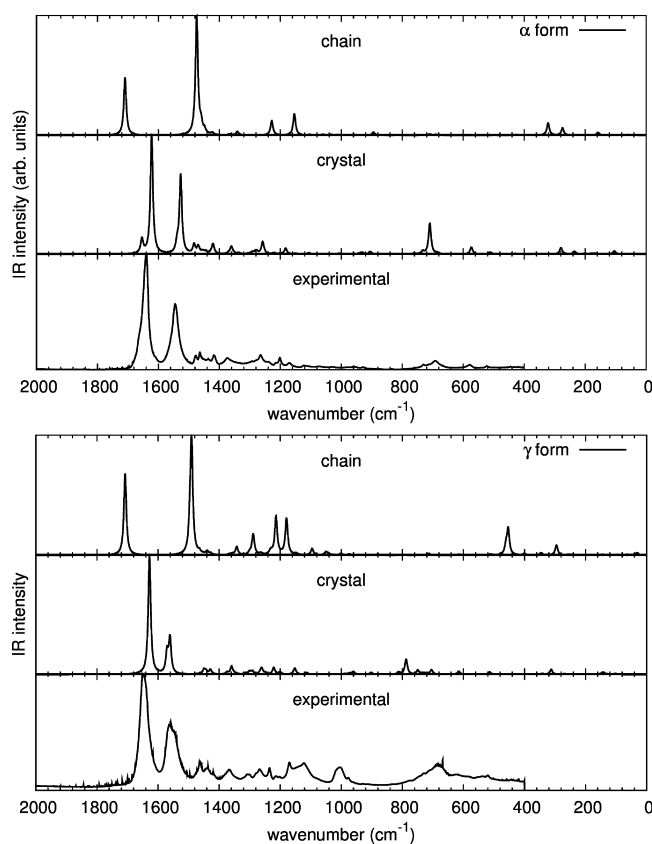

Figure 2. Comparison between experimental and DFT-D-computed IR spectra (crystal and single-chain model) for α (top) and γ (bottom) polymorphs of NY6 in the frequency range below 2000 cm^{-1} (scaling factor of 0.9614 for the whole range of frequencies).

polymorphs are shown in the range below 2000 cm^{-1}; in the same figure, IR spectra calculated for the two isolated chains, characterized by the regular conformations of the α and γ forms, are also reported for comparison. The general pattern of the experimental spectra, dominated by the so-called amide I and amide II bands in the range between 1700 and 1500 cm^{-1}, is well reproduced by DFT-D predictions on crystals. Moreover, as expected, it is immediately clear that calculations on the isolated chains are inadequate even to give a qualitative prediction of the most relevant spectral features.

Below 1500 cm^{-1}, the experimental spectra show several weaker transitions that were found to be very sensitive to the polymorph structure: These IR bands have been indeed proposed in the past as spectroscopic markers to recognize the presence of the different crystalline forms in real samples (see a list of the experimental frequencies of the most widely

used markers, proposed or employed by several authors, in Table 3).

Table 3. Frequencies of the Most Important Experimentally Determined IR Marker Bands of the α and γ Polymorphs of NY6 Previously Proposed in the Literature[3i,5,6]

	frequencies (cm^{-1})
α form	930, 950, 960, 1030, 1200
γ form	915, 970, 1002
amorphous	985, 1124
reference	1170, 1630

In the following sections (see Figures 3 and 4), a detailed discussion of the marker bands is carried out focusing on each
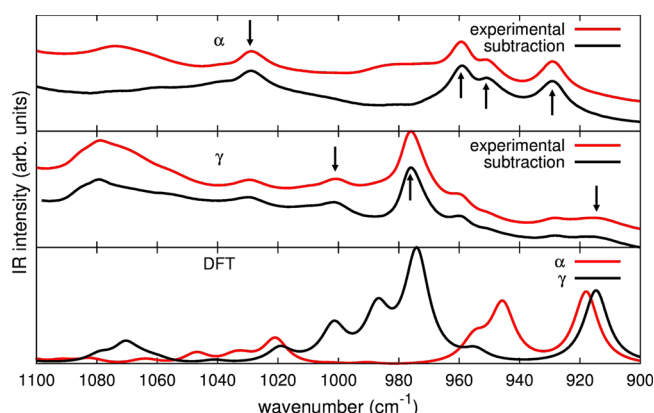
Figure 3. Comparison between experimental and DFT-D-computed IR spectra for α and γ polymorphs of NY6 in the wavenumber range 1100−900 cm^{-1} (scaling factor = 0.975). For the experimental spectra, the spectra obtained upon subtraction of the spectrum of an amorphous sample are also reported.
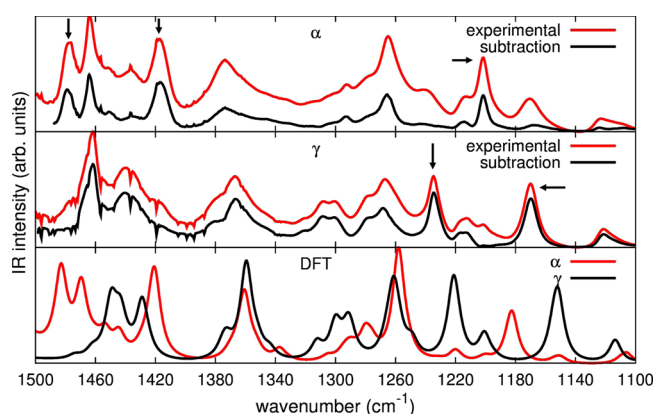

Figure 4. Comparison between experimental and DFT-D-computed IR spectra for α and γ polymorphs of NY6 in the frequency range 1500−1100 cm^{-1} (scaling factor = 0.9614). For the experimental spectra, the spectra obtained upon subtraction of the spectrum of an amorphous sample are also reported.

specific spectral region, where transitions sensitive to the crystal structure of NY6 occur. (In the Supporting Information, similar figures are reported comparing experimental spectra with DFT-computed spectra obtained using different sets of parameters for Grimme's correction.) To ease the comparison between calculations and experiments, a suitable scaling factor was employed for each spectral range; for the same reason, in the

text, we refer to calculated peak frequencies, reporting values after scaling.

900−1100 cm^{-1} Frequency Range. In Figure 3, we report a comparison between experimental and DFT-D-computed spectra for the α and γ polymorphs in the 900−1100 cm^{-1} range. This is probably the most important range because of the presence of very popular marker bands of the two polymorphs.

Indeed, according to Table 3, there are three strong marker bands for the α form at 930, 960, and 1030 cm^{-1} and two marker bands for the γ form at about 970 and 1000 cm^{-1}. Minor markers are the bands at 950 and 915 cm^{-1} for the α and γ forms, respectively.

By inspection of Figure 3, one can verify that DFT-D-computed spectra show a good agreement with the experimental ones: In particular, calculations confirm that the previously reported bands are all characteristic markers of the α and γ polymorphs of NY6.

Despite the general agreement between theory and experiments, there are several discrepancies in the description of some details: In the case of the α crystal, the predicted intensity ratios between the three bands at 930, 950, and 960 cm^{-1} do not exactly parallel the experimental ones. It should be noted that the experimental spectrum is affected by the presence of non-negligible contributions from the amorphous phase, which is indeed responsible for a broad band peaked at about 985 cm^{-1}. To obtain spectra free from the amorphous contribution, a spectral subtraction of this contribution was carried out (Figure 3) to determine whether the intensities of the two bands, in particular the 960 cm^{-1} band, could be affected. No changes were observed, and thus one can conclude that DFT-D calculations are not sufficiently accurate in this case to satisfactorily reproduce the experimental intensities and intensity ratio of the two bands.

A similar situation was found in the case of the IR spectra of the γ form (Figure 3): A good description was obtained for the bands at 970 and 1000 cm^{-1}, but an additional absorption feature was calculated between these two features. This extra transition probably falls under the main band (occurring at 970 cm^{-1} in the experimental spectrum) or shows a negligible intensity in the experiment, whereas its relative position and/or intensity are differently predicted by DFT-D calculations. It should be noted that the calculations correctly predict the existence of a third band (experimental frequency = 915 cm^{-1}), although it is again too intense with respect to the experimental (broad) band.

Despite the discrepancies underlined above, the overall agreement between the experimental and DFT-D-computed spectra is good and confirms the assignments (reported in Table 3), based on purely experimental investigations. In particular, the selectivity of this spectral region for the recognition of the two different crystalline polymorphs is well reproduced by calculations.

1100−1500 cm^{-1} Frequency Range. In Figure 4, we report a comparison between experimental and DFT-D-computed IR spectra in the frequency range of 1100−1500 cm^{-1}.

Vasanthan and co-workers[5c,6f] proposed the band at 1200 cm^{-1} as a marker of the α form, whereas no other marker bands of NY6 polymorphs have been discussed in this range so far. Based on the experimental spectra reported in Figure 4, one can see that the band falling at 1170 cm^{-1} (usually taken as a reference band[5c,e]) is predominant for the γ form, and a similar behavior was observed for the band at 1234 cm^{-1}. On this basis, we suggest that these two bands be considered as additional

markers of the γ polymorph. Moreover, in the case of the α form, in addition to the 1200 cm⁻¹ absorption, two strong bands falling at 1416 and 1478 cm⁻¹ were distinctly observed and can be thus proposed as further marker bands.

Considering DFT-D-computed spectra, the agreement with the experimental spectra was very good also in minor details. Considering first the γ form, we confirm that the experimental band at 1170 cm⁻¹ (predicted at lower frequency by the calculations, i.e., 1152 cm⁻¹) is indeed a marker of this form. This finding allows us to solve one of the discrepancies found in the literature: Indeed, the 1170 cm⁻¹ band was taken by some authors as a marker of the amorphous phase, whereas Vasanthan and Salem[5c,e] demonstrated that this band was somehow dependent on the crystal morphology of the system and proposed it as a reference band. Our results further suggest that the 1170 cm⁻¹ band can indeed be associated with the γ polymorph. Also, in the case of the band at 1234 cm⁻¹, the calculations (predicted band frequency at 1222 cm⁻¹) support its assignment to the γ form: To our knowledge, this band has not yet been proposed as a marker of the γ form. Moreover, computed data predict a further marker for this form at about 1380 cm⁻¹, where a band is clearly detected. However, in this range, the experimental spectra are quite broad and structureless, and thus, this marker band seems to be unsuitable for practical applications.

Considering the α form, DFT-D calculations confirm again that the band at 1200 cm⁻¹ is a marker band of this polymorph; moreover, calculations indicate that the two bands at 1416 and 1478 cm⁻¹ are additional markers of α form, although they have not been used for practical purposes. In addition to the main features described above, the calculations also reproduce minor details quite well, such as the pattern of bands observed between 1400 and 1500 cm⁻¹ for both forms or the pattern observed at about 1300 cm⁻¹ for the γ form.

Other Spectral Regions. In the previous section, the most relevant spectral regions for the application of IR spectroscopy to the characterization of materials based on NY6 were analyzed. In this section, we briefly discuss other different frequency ranges, where some additional information can be obtained. All of the related figures can be found in the Supporting Information.

Between 1500 and 1800 cm⁻¹ (upper panel of Figure S7, Supporting Information), the most intense vibrations of polyamides can be found, namely, the amide I and amide II bands. The relative positions observed in the experimental spectra for the two bands were reproduced correctly by DFT-D calculations. In particular, the amide I band of the α form exhibited a lower frequency than the γ form, indicating that, in the former case, there is a more efficient hydrogen-bond network, characterized by stronger bonds.

Another feature directly related to hydrogen bonding is the NH stretching band falling at about 3300 cm⁻¹ (see the lower panel of Figure S7, Supporting Information). Whereas the experimental spectra of the two polymorphs show very similar peak positions for these broad bands, DFT-D calculations predict a slightly lower frequency for the γ form, thus suggesting that stronger hydrogen bonds are present. This finding is in contrast with what is observed for the amide I band, in both the experimental and DFT-D-computed spectra. However, the fact that, considering the experimental spectra, no significant differences between the two polymorphs were found in the NH stretching region suggests that the trend given by the present calculations should be ascribed to some weaknesses of

the theoretical modeling, such as the influence of basis set superposition error or of the Grimme corrections in the description of hydrogen bonding. Furthermore, anharmonicities can have a non-negligible effect in this frequency range but were not taken into account in the present (harmonic) calculations.

Below 900 cm⁻¹, no important features were observed except for an intense and broad band at about 690 cm⁻¹ for both forms (see Figure S8, Supporting Information). Also, in this range, DFT-D calculations reproduce the experimental pattern, and in particular, they describe well the weak bands occurring between 500 and 650 cm⁻¹. However, considering the intense absorption feature falling at about 690 cm⁻¹ in both the experimental spectra, a too-large frequency splitting between the absorption peaks of the two crystalline forms is predicted by the calculations. To better clarify the origin of this discrepancy, further experimental investigations are required to clearly distinguish the contribution due to the amorphous domains in this frequency range.

Finally, in the CH stretching frequency region (Figure S9, Supporting Information), an overall agreement was found again with DFT-D calculations, despite the fact that anharmonic effects, overtones, Fermi resonances, and so on, usually significantly affect the spectral pattern. In particular, the two main broad bands of the γ form were found at lower frequencies than the two broad bands of the α form, as reproduced by DFT-D calculations. A qualitative interpretation of this fact can be proposed: It is indeed believed that, in the α form, the best geometrical arrangement for the hydrogen bonds is obtained at the expense of a less favorable packing of the >CH₂ groups of adjacent chains, whereas the opposite situation is found in the case of the γ form. The fact that the CH stretchings of the α form show higher frequencies can be ascribed to repulsive intermolecular interactions originating in the tight contact of nonbonded H atoms of the methylene units of adjacent chains. By comparing the calculated IR spectra of the crystals with those of the single chains, we verify in section IV that this behavior is indeed uniquely related to the intermolecular interactions between closely packed chains in the crystal.

IV. DISCUSSION

An additional advantage of ab initio calculations of vibrational spectra relies on the possibility to associate with each frequency (i.e., eigenvalue) the related eigenvector describing the normal mode of vibration, to carry out a band assignment. In the case of polyamides, the vibrational assignment was derived in the past only on the basis of empirical correlations or considering the eigenvectors obtained through semiempirical calculations on small oligomers.[8a,b]

In addition to the identification of characteristic group frequencies, the analysis of the computed vibrational eigenvectors allows information to be gathered on the dynamics of the system in terms of relevant intramolecular interactions and provides a tool to estimate the effect of the intermolecular interactions between different molecules. However, in the case under study, the eigenvector analysis carried out by means of a visual inspection of the Cartesian atom displacements associated with the vibrational modes of the crystal is rather difficult, because of the presence of more than one molecule per unit cell.

In this case, a useful technique for the analysis of eigenvectors is the comparison between the vibrational

Table 4. Correspondence between the Normal Modes Associated with the Main IR Transitions of the α Polymorph of NY6 and Normal Modes of the One-Dimensional Model Chain in α-Type Conformation[a,b]

crystal			isolated chain (1D model chain)				crystal			isolated chain (1D model chain)			
Freq. (cm⁻¹)	IR intens. (km/mol)	Symm. species	Freq. (cm⁻¹)	IR intens. (km/mol)	Symm species	Eigenvector	Freq. (cm⁻¹)	IR intens. (km/mol)	Symm. species	Freq (cm⁻¹)	IR intens. (km/mol)	Symm species	Eigenvector
918 (M)[c]	96 [24]	A	907	22	A₁		1337	48 [12]	B	1316	2	B₁	
946 (M)	70 [18]	B	931	1	B₁		1361	274 [69]	A	1341	26	A₁	
955 (M)	21[7]	B	948	3	B₂					1352	0 (0.2)	A₁	
1021 (M)	35 [9]	B	1009	0 (0.06)	B₁		1421 (M)	326 [81]	B	1424	7	B₁	
1106	42 [14]	A	1104	6	A₁		1444	81[20]	A	1441	0 (0.03)	A₁	
1182 (M)	179 [45]	A	1155	153	A₁		1454	73[18]	B	1441	1	B₁	
1185	45 [11]						1469	243[61]	B	1479	2	B₁	
1258	462 [115]	A	1228	105	A₁		1483(M)	157 [39]					
1276	48[12]	A	1259	0	A₂		1482	57 [14]	A	1479	13	A₁	
1280	100[25]	A	1261	0 (0.5)	A₁		1482	43 [11]	B	1479	5	B₁	
							1484	60 [15]					

[a]Frequencies scaled by 0.9614 (above 1100 cm⁻¹) and 0.975 (below 1100 cm⁻¹). [b]IR intensity values normalized to the number of chains in the unit cell of the crystal in brackets. [c]Marker bands are indicated by (M).

modes calculated for the single, regular chain (one-dimensional model chain) and the vibrational modes of the crystal. In this way, it is possible to establish a correspondence between the latter and the former, which provides a description of the vibrational problem of the crystal on the basis of the vibrational modes of the isolated chain. Moreover, it allows the effects of the intermolecular interactions in terms of frequency shifts and IR intensity redistributions driven by the different vibrational couplings occurring in the single chain with respect to the crystal to be captured. Indeed, in the presence of strong intermolecular interactions, the description (in terms of atomic displacements) of the vibrational modes of the crystal can markedly deviate from that of any mode of the isolated chain. This behavior is often found in the case of NY6 and explains the impressive change of the spectral pattern when intermolecular interactions are taken into account.

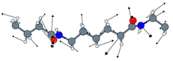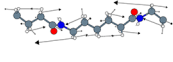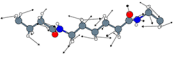The detailed analytical procedure followed to carry out this analysis is reported in the Supporting Information.
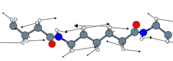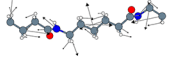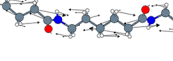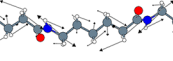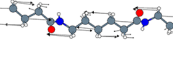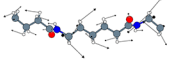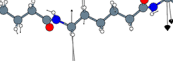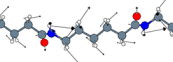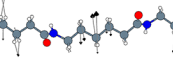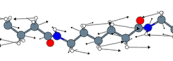
The method was applied to the analysis of the marker bands discussed in the previous sections: the correlation established between the normal modes of the crystal and those of the one-dimensional model chain is illustrated in Tables 4 and 5, where frequencies and IR intensities of selected transitions of the α and γ crystals are shown. The data here reported were extracted

from the output of the DFT-D calculations according to the following criteria:

(a) All IR transitions previously identified as markers (or potential markers) for the detection of the crystal polymorphs are reported.

(b) Strong IR features (even if not recognized as marker bands) in the characteristic range 1500−900 cm⁻¹ are included in the tables. In this case, a quite drastic threshold intensity value of 40 km/mol was defined, corresponding to about 10% of the strongest IR transition of the α form in this frequency range.
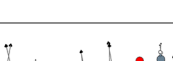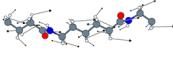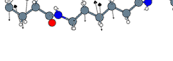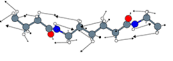
(c) For any given selected transition of the crystal, we report the computed (scaled) frequency and intensity of the corresponding (i.e., similar) IR transition of the isolated chain (one-dimensional model chain). This normal mode of the single chain is the one showing the higher similarity to the normal mode of the crystal considered (i.e., it shows the highest scores $s_{kt}^{(i)}$; see the Supporting Information). A sketch of the eigenvector (single-chain mode) is also reported, thus providing an indication useful for the vibrational assignment.

According to the symmetry rules dictated by the site symmetry, the vibrations of the crystal showing correspondence with vibrations of the one-dimensional model chain must obey the following symmetry relationships:

Table 5. Correspondence between the Normal Modes Associated with the Main IR Transitions of the γ Polymorph of NY6 and the Normal Modes of the One-Dimensional Model Chain in γ-Type Conformation[a,b]

crystal			isolated chain (1D model chain)				crystal			isolated chain (1D model chain)			
Freq (cm⁻¹)	IR intens. (km/mol)	Symm. species	Freq (cm⁻¹)	IR intens. (km/mol)	Symm species	eigenvector	Freq (cm⁻¹)	IR intens. (km/mol)	Symm. species	Freq (cm⁻¹)	IR intens. (km/mol)	Symm species	eigenvector
915 (M)[c]	49 [25]	B$_u$	893	4	B		1291 1300	51 [26] 74 [37]	A$_u$	1288	89	A	
974 (M)	73 [37]	B$_u$	962	1	B					1291	12	A	
1002 (M)	23 [12]	B$_u$	996	1	B		1360	192 [96]	A$_u$	1342	39	A	
1113	48 [20]	A$_u$	1096	30	A					1354	4	A	
1152 (M)	121 [61]	B$_u$	1150	7	B		1429	116 [58]	B$_u$	1438	13	B	
1155	51 [26]	A$_u$	1142	1	A		1443	81 [41]	B$_u$	1444	0 (0.38)	B	
1201	55 [28]	B$_u$	1197	3	B		1449	102 [61]	B$_u$	1465	11	B	
1222 (M)	153 [77]	A$_u$	1214	183	A								
1262	135 [68]	A$_u$	1229	14	A								

[a]Frequencies scaled by 0.9614 and 0.975 above and below 1100 cm⁻¹, respectively. [b]IR intensity values normalized to the number of chains in the unit cell of the crystal in brackets. [c]Marker bands are indicated by (M).

(a) For the α form, the A and B modes can be obtained as mixing of A$_1$, A$_2$ and B$_1$, B$_2$ modes, respectively, of the α-type isolated chain.

(b) For the γ form, the A$_u$ and B$_u$ modes are obtained from A and B modes, respectively, of the γ-type chain.

Notice that, to make a correct comparison between IR band intensities obtained for crystals and one-dimensional model chains, the IR intensity values of the crystals must be divided by the number of chains in the unit cell (values in brackets in Tables 4 and 5).

IV.1. IR Spectra of Crystals and Isolated Chains. Before performing a detailed analysis of the data reported in Tables 4 and 5, it is instructive to compare the predicted IR features of the isolated chains and of crystals, reported in Figure 5. To carry out a correct comparison, the intensity relative to crystals must be normalized to the number of chains belonging to the crystal cell.

Considering the 1100−800 cm⁻¹ range, the most impressing effect due to the three-dimensional arrangement of the chains is a marked increase of the global intensity. In particular, in the case of the α form, the IR spectrum of the isolated chain presents just one strong infrared active band (at 907 cm⁻¹), whereas in the spectrum of the crystal, at least two strong features appear with comparable intensity. Interestingly, a frequency correlation seems to exist between the band of the one-dimensional model chain at 907 cm⁻¹ and the lower-frequency band of the crystal (918 cm⁻¹), which moreover shows a very similar intensity. The situation is even more dramatic for the γ form, where several relevant features appear in the crystal, whereas the single chain shows only two features (at 1056 and 1096 cm⁻¹) of medium intensity.

In the range of 1500−1100 cm⁻¹, neglecting the strong amide II transition that appears between 1400 and 1500 cm⁻¹ for the isolated chains and is affected by a marked blue shift in the crystal (see Figure 2) due to the occurrence of H bonding, it is very difficult to establish a correspondence between the IR bands of the crystals and those of the isolated chains. It seems that, in this range, the global intensity is only slightly enhanced by the crystal packing, but it is redistributed over a larger number of vibrational modes, giving rise to very structured spectra.

The data reported in Tables 4 and 5 are useful to rationalize these trends.

By considering the sketches of the eigenvectors of the single isolated chains (last column of Tables 4 and 5), all of the vibrational modes can be labeled as collective normal modes, because they involve cooperative angular deformations of all the CH$_2$ units and, in most cases, also contain a non-negligible contribution by bending of the amide groups. The "delocalization" of these modes over all of the chemical groups of the polymer chains does not allow a classification in terms of characteristic group vibrations. On the other hand, this clearly explains why the spectral ranges considered are so sensitive both to the chain conformation and to the crystal packing: It is
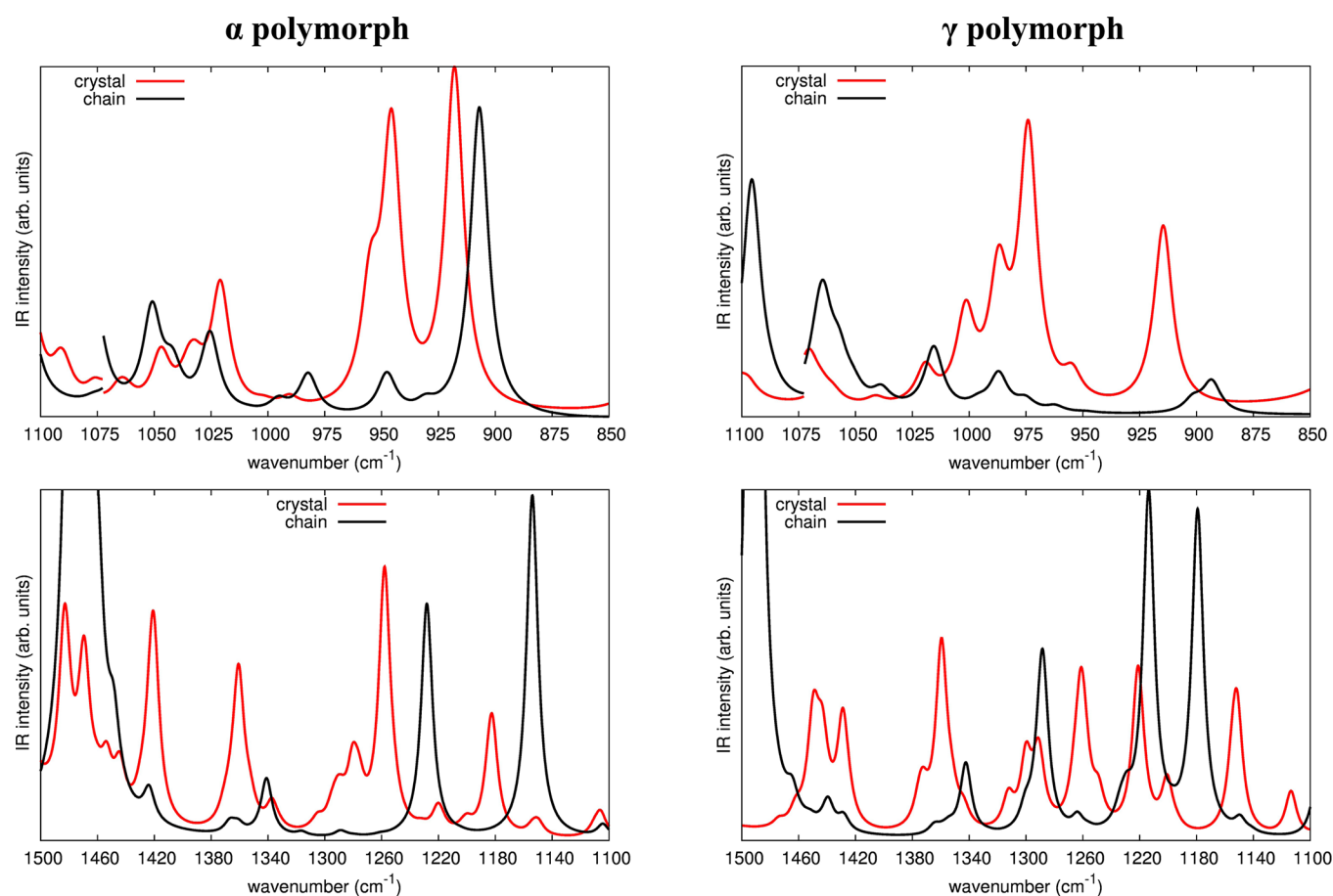
Figure 5. Comparison between DFT-D-computed IR spectra of the crystal and one-dimensional model chain of the α (left) and γ (right) polymorphs of NY6 in the frequency ranges $900-1100$ cm^{-1} (frequency scaling factor = 0.975) and $1500-1100$ cm^{-1} (frequency scaling factor = 0.9614). For a correct comparison, the intensities of the crystals were divided by the number of chains in the unit cell. The discontinuities at about 1075 cm^{-1} are due to the use of different scaling factors.

indeed well-known that frequencies of collective normal modes are usually strongly affected by the specific molecular shape, that is, by the architecture of the molecule as a whole.

Another remark can be made about the calculated frequencies of the crystal and the corresponding ones of the isolated chain: Frequencies of the two similar modes are quite close, and in most cases, the relative shifts do not exceed 20 cm^{-1}. Nevertheless, there is a remarkable remixing of the single-chain modes considering the vibrations of the crystal structures. This is especially true in the higher frequency range, where the analysis of the score values demonstrates that many vibrations of the crystal take comparable contributions (i.e., comparable score values) from many vibrations of the isolated chain.

Considering the IR intensity values reported in Tables 4 and 5, it can be seen that totally symmetric vibrations (i.e., modes invariant under the symmetry operation associated with the 2-fold screw axis) show a different behavior than vibrations belonging to the B species. Indeed, the transitions of the one-dimensional model chains associated with totally symmetric modes show the highest IR intensities, whereas those of B species are usually very weak. In the crystal, there is a general increase of the intensity associated with B-symmetry normal modes, which in several cases, show an intensity enhancement of about 1 order of magnitude with respect to the corresponding transition (similar normal mode) of the isolated chain. On the other hand, normal modes of A-symmetry species can show the following different behaviors:

(a) The IR intensity of the normal mode of the chain can be almost "transferred" to the similar mode of the crystal (consider, for instance, the modes of the α crystal at 918, 1258, and 1482 cm^{-1}).

(b) The IR intensity of the normal modes of the isolated chain can show a non-negligible decrease while going to the similar ones of the crystal; in this case, the intensity decrease seems to be compensated by an intensity enhancement of other normal modes of the crystal, just belonging to the A species. As an example, the 1182 and 1185 cm^{-1} bands of the α crystal show a total IR intensity of 56 km/mol (per chain) to be compared with the intensity (153 km/mol) of the similar mode of the single chain at 1155 cm^{-1}. This intensity depletion in the crystal is partially compensated by the occurrence of the 1280 cm^{-1} band (25 km/mol), correlated with a weakly IR-active A_1 mode of the single chain (0.5 km/mol) at 1261 cm^{-1}. This last feature can be simply ascribed to the effect of mode remixing occurring in the crystal, as confirmed by considering the whole set of scores obtained.

As a further support for the above conclusions, some summary data are reported in Table 6, where the intensity behavior of the infrared spectrum of one-dimensional model chains and crystals of NY6 (α and γ forms) is illustrated on the basis of global IR intensity values, obtained as sums of the

Table 6. Intensity Behavior of the Infrared Spectra of One-Dimensional Model Chains (Single Chains) and Crystals of NY6 in the α and γ Forms[a,b]

		α Form of NY6			
		IR intensity (km/mol)			
		A		B	
frequency range (cm⁻¹)	modes selected	1-D (chain)	3-D (crystal)[c]	1-D (chain)	3-D (crystal)[c]
900−1150	most intense + markers	28	138 [35]	4	125 [31]
	all	45	181 [45]	12	169 [42]
1150−1550	most intense + markers	296	1247 [311]	17	1013 [253]
	all	402	1550 [388]	23	1240 [310]

		γ Form of NY6			
		IR intensity (km/mol)			
		A_u		B_u	
frequency range (cm⁻¹)	modes selected	1-D (chain)	3-D (crystal)[c]	1-D (chain)	3-D (crystal)[c]
900−1150	most intense + markers	30	48 [24]	6	145 [72]
	all	59	83 [41]	20	189 [95]
1150−1550	most intense + markers	341	657 [328]	34	475 [238]
	all	511	784 [392]	91	692 [346]

[a]Data refer to sum of the IR intensities of selected transitions belonging to given spectral ranges (see text for details). [b]Contributions from normal modes of symmetry species A and B presented separately. [c]IR intensity values normalized to the number of chains in the unit cell of the crystal in brackets.

intensities of the selected transitions analyzed in Tables 4 and 5. In Table 6, contributions from normal modes of the symmetry species A and B are presented separately. It can immediately be realized that the total intensity associated with the totally symmetric vibrations of the single chain is practically kept unaltered in the crystal, whereas B modes undergo to a marked intensity enhancement in the crystal. To confirm that this peculiar behavior is related neither to the (quite arbitrary) selection of bands made in Tables 4 and 5 nor to the selection of the normal modes of the one-dimensional model chain (based on the similarity criterion), we show in Table 6 IR intensity data obtained by summing over the whole spectral ranges analyzed in Tables 4 and 5, without any preliminary selection of bands for crystals and one-dimensional model chains. These data confirm the trends already described, for both the α and γ polymorphs.

Accordingly, it seems quite clear that the strong intermolecular interactions arising from the formation of interchain H bonds selectively affect the IR intensity of normal vibrations transverse with respect to the chain axis (i.e., B normal modes), as expected because of the geometrical arrangement of the H bonds. An extended and deeper analysis based on internal and Cartesian intensity parameters[25] would be required to give further insights into this behavior.

IV.2. Classification of the Marker Bands: Crystallinity and Regularity Bands. Tables 4 and 5 demonstrate that most of the marker bands of both polymorphs are true markers of crystallinity: they are indeed associated with modes that show negligible intensities for the single one-dimensional models but gain intensity due to the interactions occurring in the crystal.

On the other hand, some bands (e.g., the bands at 918 and 1182 cm⁻¹ for the α form and those at 1113 and 1222 cm⁻¹ for the γ form, all of A species) show similar or even lower (normalized) intensities in the crystal than in the polymer chain. These bands can be considered specific markers of the presence of a regular chain having a transplanar α-type or a nonplanar γ-type conformation: On one hand, they are well correlated (frequency and intensity) with vibrations of the single chain, and on the other hand, they are not affected by the characteristic intensity enhancement associated with the formation of the H bonds between the chains. For this reason, we prefer to label the above IR absorptions as "regularity bands" instead of "crystallinity bands". Notice that the experimental marker band of the α form at 930 cm⁻¹ (computed frequency of 918 cm⁻¹) found wide application in the literature for the characterization of NY6 polymorphism by means of IR spectroscopy, and its classification as a conformation-sensitive regularity band is particularly meaningful in this respect.

In Table 7, the full list of marker bands of NY6 crystal polymorphs (including the markers newly proposed in this work) is summarized.

Table 7. Classification of Marker Bands of NY6 Crystal Polymorphs

experimental frequency (cm⁻¹)	ref(s)	DFT-D-computed frequency (scaled) (cm⁻¹)	IR intensity (km/mol)	regularity/ crystallinity assignment
		α Form		
930	1b, 5, 6	918	96	regularity
950	5b, e	946	70	crystallinity
960	5a, e, b, 1b, 6e, 5f	955	21	crystallinity
1030	5e, 6e, 5f	1021	35	crystallinity
1200	5e	1182	179	regularity
1416		1421	326	crystallinity
1478		1483	157	crystallinity
		γ Form		
915	5a, 6e, 5f	915	49	crystallinity
970	1b, 5, 6a−d, f	974	73	crystallinity
1000	6e, 5f	1002	23	crystallinity
1170	5e	1152	121	crystallinity
1234		1222	153	regularity

IV.3. CH Stretching Region. Further insight into the role of intermolecular interactions in affecting the vibrational properties of NY6 can be obtained by comparing the IR spectra of the one-dimensional model chain and the crystal in the CH stretching region. In Figure 6, we report the computed IR spectra of the crystal and the single polymer chain for both polymorphs. The α-type and γ-type one-dimensional model chains have CH stretching bands in the same frequency range, whereas the situation is markedly different for the two crystals. This behavior was already outlined in the previous section concerning the experimental spectra, and it was attributed to the different extents of interactions between >CH_2 groups of adjacent chains in the two cases.

Figure 6 shows that, in the case of the γ form, the shape and intensity of the IR spectrum changes in going from the isolated chain to the crystal but, overall, there is not a significant frequency shift. On the contrary, in the case of the α crystal, a
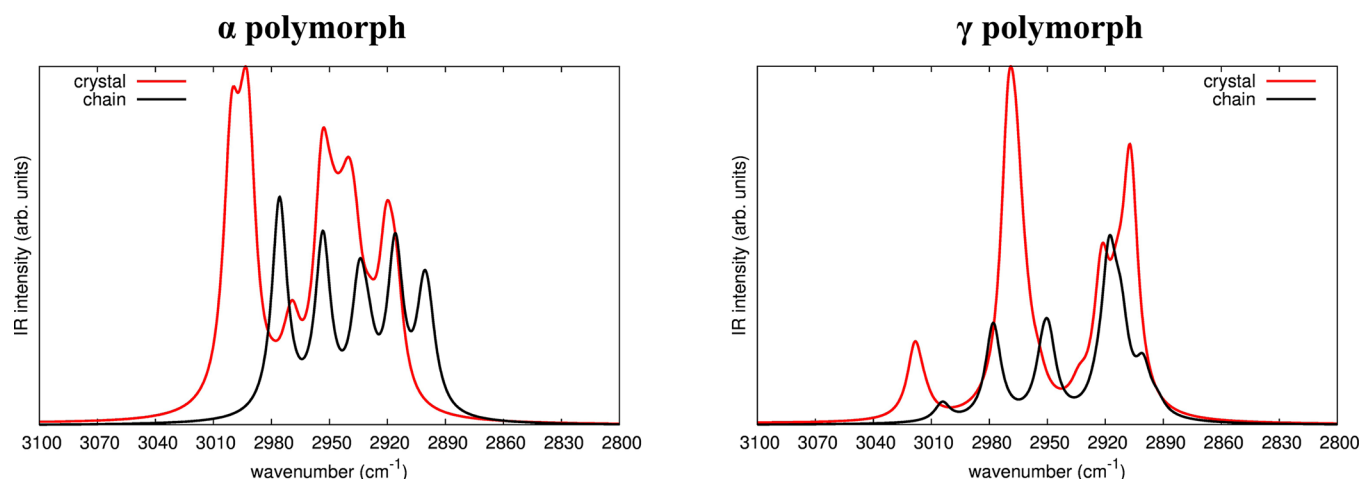
α polymorph

γ polymorph

Figure 6. Comparison between DFT-D-computed IR spectra of the crystal and one-dimensional model chain of the α (left) and γ (right) polymorphs of NY6 in the frequency range 2800−3100 cm^{-1} (frequency scaling factor = 0.9614). For a correct comparison, the intensities of the crystal were divided by the number of chains in the unit cell.

non-negligible frequency blue shift of the main peak is observed with respect to the one-dimensional model chain, thus revealing a stronger intermolecular interaction between >CH$_2$ groups of the adjacent chains in this form.

V. CONCLUSIONS

The characterization of polymer structures and of their vibrational properties by means of high-level quantum chemical approaches is only at its early stages. Whereas molecular dynamics simulations and periodic first-principles calculation have been used to investigate the crystal structures of macromolecules, very few calculations have been carried out for the determination of the vibrational spectra of polymers, because of the fact that quantum chemical calculations are required for a reliable determination of the vibrational force field. So far, DFT or ab initio calculations have been carried out by taking into account small molecular models (i.e., short oligomers), according to the so-called "oligomer approach".[26] Because of these limitations, the investigation of the vibrational properties of polymers and also the vibrational assignments of the IR spectra for practical and analytical purposes have been based so far only on purely experimental works or semi-empirical calculations, and a confirmation based on a reliable theoretical investigation is still lacking. Indeed, contrasting assignments, interpretations, and also some ambiguities are often present in the literature. Only recently, periodic ab initio calculations of IR spectra of polymers have been presented,[10,12,27] thanks in particular to the new computational tools that have been implemented and that are now routinely available in a few packages.

In this work, we used CRYSTAL09 to carry out DFT-D calculations of the IR spectra of two nylon 6 polymorphs (α and γ forms). The CRYSTAL code is particularly powerful for this purpose because of the possibility of taking into account the full symmetry of the crystal, as required for a reliable band assignment and for the subsequent investigation of the polarization properties of the system. Furthermore, van der Waals interactions can be taken into account by including Grimme's correction in DFT functionals.[15,16] The use of a Gaussian basis set further allows a quantum description of the system that is more "molecule-based" than other approaches, such as the pseudopotential plane-wave method. A good

description of the crystalline structures was obtained for both the α and γ polymorphs of NY6, and the comparison between DFT-D-computed and experimental IR spectra of the two forms supports the reliability of the method. Some marker bands previously found from experimental investigations have been confirmed and assigned. Some other assignments have been revised on the basis of the comparison between the calculated spectrum of the crystal and that of the single chain. In particular, the widely used marker bands at 930 and 1200 cm^{-1} of the α form have been confirmed to be markers of a regular transplanar conformation, not necessarily related to the occurrence of a crystal packing. We found that the band at 1170 cm^{-1}, assigned ambiguously in the literature, is peculiar of the γ form. Moreover, we have proposed some new marker bands at 1416 and 1478 cm^{-1} for the α form and at 1234 cm^{-1} for the γ form.

The results obtained demonstrate that quantum chemical calculations of the IR spectra of polymers are now viable; they can be applied to a very wide range of problems and can open the way for new applications of the modeling. Indeed, in addition to the straightforward review of the experimental assignments of the vibrational spectra of many classes of polymer, they can provide answers to several open questions. In the case of nylons, the study of the relative stability of the α or γ forms with varying length of the monomer chemical unit, the characterization of other stable crystalline forms, and the determination of the crystalline structure of nylons that have not been precisely refined based on XRD experiments are just few examples where the state-of-the-art computational techniques exploited herein could make a significant contribution.

Furthermore, an increasingly deep insight into the molecular phenomena ruling the physicochemical and mechanical performances of polymer materials is expected to be the direct outcome of these computational methodologies. In particular, these approaches can support standard characterization techniques in the study of new polymeric system, such as nanocomposites, electrospun nanofibers, and nanostructured polymer materials currently being developed for a wide number of innovative applications in many different fields.

■ ASSOCIATED CONTENT

S Supporting Information

Additional computational details, tables, and discussion of the predictions of the crystal structure. Description of the procedure for eigenvector analysis. Figures reporting comparisons between experimental and DFT-D-computed IR spectra for both the α and γ polymorphs of nylon 6 in all of the different frequency ranges and different sets of parameters for Grimme's correction. Tables of DFT-D-computed frequencies and intensities of α/γ crystals and α-type/γ-type one-dimensional model chains obtained for different sets of parameters in Grimme's correction. Tables of DFT-D-computed cell parameters and fractional coordinates of α and γ crystals obtained for different sets of parameters in Grimme's correction. Table of score values for the eigenvector analysis of the vibrational modes of the two NY6 polymorphs. This material is available free of charge via the Internet at http://pubs.acs.org.

■ AUTHOR INFORMATION

Corresponding Author
*E-mail: alberto.milani@polimi.it.

Notes

The authors declare no competing financial interest.

■ REFERENCES

(1) (a) Loo, L. S.; Gleason, K. K. *Macromolecules* **2003**, *36*, 2587−2590. (b) Chen, G.; Shen, D.; Feng, M.; Yang, M. *Macromol. Rapid Commun.* **2004**, *25*, 1121−1124.

(2) (a) Song, K.; Rabolt, J. F. *Macromolecules* **2001**, *34*, 1650−1654. (b) Lee, K. H.; Kim, K. W.; Pesapane, A.; Kim, H. Y.; Rabolt, J. F. *Macromolecules* **2008**, *41*, 1494−1498. (c) Granato, F.; Bianco, A.; Bertarelli, C.; Zerbi, G. *Macromol. Rapid Commun.* **2009**, *30*, 453−458. (d) Bianco, A.; Iardino, G.; Manuelli, A.; Bertarelli, C.; Zerbi, G. *Chem Phys Chem* **2007**, *8*, 510−514. (e) Stephens, J. S.; Chase, D. B.; Rabolt, J. F. *Macromolecules* **2004**, *37*, 877−881. (f) Liu, Y.; Qi, L.; Guan, F.; Hedin, N. E.; Zhu, L.; Fong, H. *Macromolecules* **2007**, *40*, 6283−6290. (g) Zussman, E.; Burman, N.; Yarin, A. L.; Khalfin, R.; Cohen, Y. *J. Polym. Sci. B: Polym. Phys.* **2006**, *44*, 1482−1489. (h) Stachewicz, U.; Barber, A. H. *Langmuir* **2011**, *27*, 3024−3029. (i) Milani, A.; Casalegno, M.; Castiglioni, C.; Raos, G. *Macromol. Theory Simul.* **2011**, *20*, 305−319.

(3) (a) Kohan, M. I. *Nylon Plastics Handbook*; Hanser: New York, 1995. (b) Kinoshita, Y. *Makromol. Chem.* **1959**, *33*, 1−19. (c) Slichter, W. P. *J. Polym. Sci.* **1959**, *36*, 259−266. (d) Ramesh, C. *Macromolecules* **1999**, *32*, 3721−3726. (e) Ramesh, C.; Gowd, E. B. *Macromolecules* **2001**, *34*, 3308−3313. (f) Murthy, N. S. *Polym. Commun.* **1991**, *32*, 301−305. (g) Salem, D. R.; Weigmann, H. D. *Polym. Commun.* **1989**, *30*, 336−338. (h) Murthy, N. S.; Minor, H. *Polym. Commun.* **1991**, *32*, 297−300. (i) Arimoto, H. *J. Polym. Sci.* **1964**, *2*, 2283−2295.

(4) (a) Aleman, C.; Casanovas. *J. Colloid Polym. Sci.* **2004**, *282*, 535−543. (b) Bernadò, P.; Aleman, C.; Puiggali, J. *Eur. Polym. J.* **1999**, *35*, 835−847. (c) Len, S.; Aleman, C.; Munoz-Guerra, S. *Macromolecules* **2000**, *33*, 5754−5756.

(5) (a) Murthy, N. S.; Bray, R. G.; Correale, S. T.; Moore, R. A. F. *Polymer* **1995**, *36*, 3863−3873. (b) Loo, L. S.; Gleason, K. K. *Macromolecules* **2003**, *36*, 6114−6126. (c) Vasanthan, N.; Salem, D. R. *J. Polym. Sci. B: Polym. Phys.* **2001**, *39*, 536−547. (d) Na, B.; Lv, R.; Tian, N.; Xu, W.; Li, Z.; Fu, Q. *J. Polym. Sci. B: Polym. Phys.* **2009**, *47*, 898−902. (e) Vasanthan, N. *J. Polym. Sci. B: Polym. Phys.* **2003**, *41*, 2870−2877. (f) Miri, V.; Persyn, O.; Lefebvre, J. M.; Segula, R.; Stroeks, A. *Polymer* **2007**, *48*, 5080−5087.

(6) (a) Miyake, A. *J. Polym. Sci.* **1960**, *44*, 223−232. (b) Sandeman, I.; Keller, A. *J. Polym. Sci.* **1956**, *19*, 401−435. (c) Rotter, G.; Ishida, H. *J. Polym. Sci. B: Polym. Phys.* **1992**, *30*, 489−495. (d) Vasanthan, N. *Appl. Spectrosc.* **2005**, *59*, 897−903. (e) Persyn, O.; Miri, V.; Lefebvre, J. M.; Depecker, C.; Gors, C.; Stroeks, A. *Polym. Eng. Sci.* **2004**, *44*, 261−271. (f) Vasanthan, N.; Murthy, N. S.; Bray, R. G. *Macromolecules* **1998**, *31*, 8433−8435.

(7) (a) Dasgupta, S.; Hammond, W. B.; Goddard, W. A. *J. Am. Chem. Soc.* **1996**, *118*, 12291−12301. (b) Li, Y; Goddard, W. A. *Macromolecules* **2002**, *35*, 8440−8455.

(8) (a) Gaigeot, M. P. *Phys. Chem. Chem. Phys.* **2010**, *12*, 3336−3359. (b) Brauer, B.; Pincu, M.; Buch, V.; Bar, I.; Smons, J. P.; Gerber, R. B. *J. Phys. Chem A* **2011**, 5859−5872. (c) Pagliai, M.; Cavazzoni, C.; Cardini, G.; Erbacci, G.; Parrinello, M.; Schettino, V. *J. Chem. Phys.* **2008**, *128*, 224514.

(9) (a) Jakes, J.; Krimm, S. *Spectrochim. Acta A* **1971**, *27*, 19−34. (b) Jakes, J.; Krimm, S. *Spectrochim. Acta A* **1971**, *27*, 35−63. (c) Shukla, S. K.; Kumar, N.; Tandom, P.; Gupta, V. D. *J. Appl. Polym. Sci.* **2010**, *116*, 3202−3211.

(10) (a) Dovesi, R.; Saunders, V. R.; Roetti, C.; Orlando, R.; Zicovich-Wilson, C. M.; Pascale, F.; Civalleri, B.; Doll, K.; Harrison, N. M.; Bush, I. J.; D'Arco, P.; Llunell, M. *CRYSTAL09 User's Manual*; University of Torino: Torino, Italy, 2009. (b) Dovesi, R.; Orlando, R.; Civalleri, B.; Roetti, C.; Saunders, V. R.; Zicovich-Wilson, C. M.; Pascale, F.; Civalleri, B. *Z. Kristallogr.* **2005**, *220*, 571−573.

(11) (a) Javier Torres, F.; Civalleri, B.; Meyer, A.; Musto, P.; Albunia, A. R.; Rizzo, P.; Guerra, G. *J. Phys. Chem. B* **2009**, *113*, 5059−5071. (b) Javier Torres, F.; Civalleri, B.; Pisani, C.; Musto, P.; Albunia, A. R.; Guerra, G. *J. Phys. Chem. B* **2007**, *111*, 6327−6335. (c) Albunia, A. R.; Rizzo, P.; Guerra, G.; Javier Torres, F.; Civalleri, B.; Zicovich-Wilson, C. M. *Macromolecules* **2007**, *40*, 3895−3897.

(12) Ferrari, A. M.; Civalleri, B.; Dovesi, R. *J. Comput. Chem.* **2010**, *31*, 1777−1784.

(13) (a) Noel, Y.; D'Arco, P.; Demichelis, R.; Zicovich-Wilson, C. M.; Dovesi, R. *J. Comput. Chem.* **2010**, *31*, 855−862. (b) Zicovich-Wilson, C. M.; Kirtman, B; Civalleri, B.; Ramirez-Solis, A. *Phys. Chem. Chem. Phys.* **2010**, *12*, 3289−3293. (c) Colle, R.; Grosso, G.; Ronzani, A.; Zicovich-Wilson, C. *Phys. Status Solidi B* **2011**, *6*, 1360−1368.

(14) (a) Becke, A. D. *J. Chem. Phys.* **1993**, *98*, 5648−5652. (b) Lee, C.; Yang, W.; Parr, R. G. *Phys. Rev. B* **1988**, *37*, 785−789.

(15) (a) Grimme, S. *J. Comput. Chem.* **2004**, *25*, 1463−1473. (b) Grimme, S. *J. Comput. Chem.* **2006**, *27*, 1787−1795.

(16) Civalleri, B.; Zicovich-Wilson, C. M.; Valenzano, L.; Ugliengo, P. *CrystEngComm* **2008**, *10*, 405−410.

(17) (a) Bondi, A. *J. Phys. Chem.* **1964**, *68*, 441−451. (b) Rowland, R. S.; Taylor, R. *J. Phys. Chem.* **1996**, *100*, 7384−7391.

(18) (a) Holmes, D. R.; Bunn, C. W.; Smith, D. J. *J. Polym. Sci.* **1955**, *17*, 159−177. (b) Simon, P.; Argay, G. Y. *J. Polym. Sci. B: Polym. Phys.* **1978**, *16*, 935−937.

(19) Arimoto, H.; Ishibashi, M.; Hirai, M. *J. Polym. Sci. A: Polym. Chem.* **1965**, *3*, 317−326.

(20) (a) Painter, P. C.; Coleman, M. M.; Koening, J. L. *The Theory of Vibrational Spectroscopy and Its Application to Polymeric Materials*; Wiley: Chichester, U.K., 1982. (b) Zerbi, G. In *Advances in Infrared and Raman Spectroscopy*; Clark, R. J. H., Hester, R. R., Eds.; Wiley: New York, 1984; Vol. *11*, p 301. (c) Castiglioni, C. In *Vibrational Spectroscopy of Polymers: Principles and Practices*; Everall, N. J., Chalmers, J. M., Griffiths, P. R., Eds.; Wiley: Chichester, U.K., 2007; p 455.

(21) Merrick, J. P.; Moran, D.; Radom, L. *J. Phys. Chem. A* **2007**, *111*, 11683−11700.

(22) Dendena, M. *Master's Thesis*, Politecnico di Milano, Milano, Italy, 2010.

(23) Abu-Isa, I. A. *J. Appl. Polym. Sci.* **1971**, *15*, 2865−2876.

(24) Itho, T. *Jpn. J. Appl. Phys.* **1976**, *15*, 2295−2306.

(25) (a) Gussoni, M.; Castiglioni, C.; Zerbi, G. In *Handbook of Vibrational Spectroscopy*; Chalmers, J., Griffiths, P., Eds.; John Wiley & Sons: Chichester, U.K., 2001; pp 2040−2077. (b) Milani, A.; Castiglioni, C. *J. Phys. Chem. A* **2010**, *114*, 624−632. (c) Milani, A.; Galimberti, D; Castiglioni, C.; Zerbi, G. *J. Mol. Struct.* **2010**, *976*, 342−349. (d) Milani, A.; Tommasini, M.; Castiglioni, C. *Theor. Chem. Acc.* **2012**, *131*, 1139.

(26) (a) Koglin, E.; Meier, R. J. *Comput. Theor. Polym. Sci.* **1999**, *9*, 327−333. (b) Meier, R. J. *Polymer* **2002**, *43*, 517−522. (c) Tarazona, A.; Koglin, E.; Coussens, B. B.; Meier, R. J. *Vib. Spectrosc.* **1997**, *14*, 159−170. (d) Milani, A.; Castiglioni, C.; Di Dedda, E.; Radice, S.; Canil, G.; Di Meo, A.; Picozzi, R.; Tonelli, C. *Polymer* **2010**, *51*, 2597−2610. (e) Milani, A.; Tommasini, M.; Castiglioni, C.; Zerbi, G.; Radice, S.; Canil, G.; Toniolo, P.; Triulzi, F.; Colaianna, P. *Polymer* **2008**, *49*, 1812−1822. (f) Milani, A.; Zanetti, J.; Castiglioni, C.; Di Dedda, E.; Radice, S.; Canil, G.; Tonelli, C. *Eur. Polym. J.* **2012**, *48*, 391−403.

(27) (a) Nakhmanson, S. M.; Korlacki, R.; Travis Johnston, J.; Ducharme, S.; Ge, Z.; Takacs, J. M. *Phys. Rev. B* **2010**, *81*, 174120. (b) Kleis, J.; Lundqvist, B. I.; Langreth, D. C.; Schroder, E. *Phys. Rev. B* **2007**, *76l*, 100201. (c) Ramer, N. J.; Marrone, T.; Stiso, K. A. *Polymer* **2006**, *47*, 7160−7165. (d) Ramer, N. J.; Raynor, C. M.; Stiso, K. A. *Polymer* **2006**, *47*, 424−428.